Electronic Supplementary Information (ESI)

Chemical micromotors self-assemble and self-propel by spontaneous symmetry breaking

Tingting Yu,‡[ab] Prabha Chuphal,‡[c] Snigdha Thakur,[c] Shang Yik Reigh,*[a] Dhruv P. Singh*[a] and Peer Fischer*[ab]

[a] Max Planck Institute for Intelligent Systems, Heisenbergstr. 3, 70569 Stuttgart, Germany
[b] Institute of Physical Chemistry, University of Stuttgart, Pfaffenwaldring 55, 70569 Stuttgart, Germany
[c] Department of Physics, Indian Institute of Science Education and Research, Bhopal, India

*Email: reigh@is.mpg.de, dhruvpsingh@is.mpg.de, fischer@is.mpg.de

Table of Contents

Supplementary Information: Experiments

Supplementary Information: Experiments

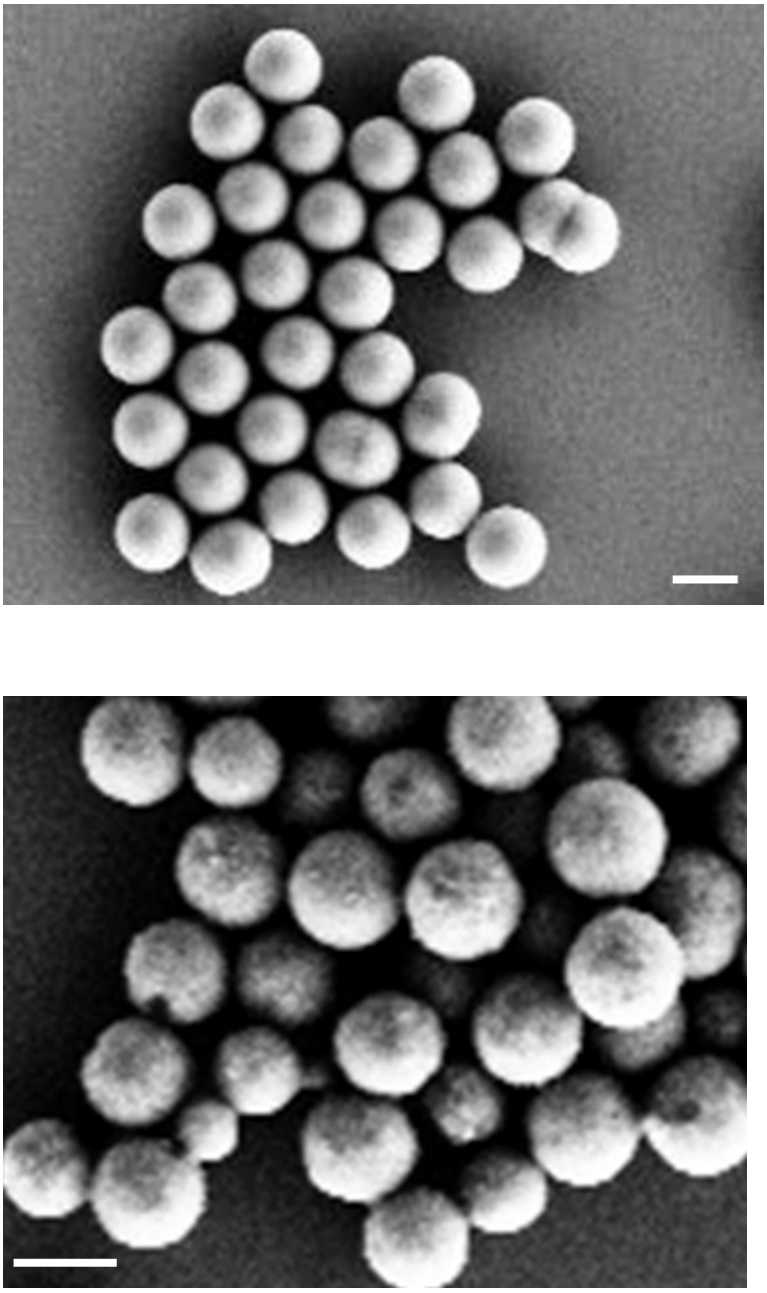

Figure S1. (Top) SEM image of 2 μm diameter SiO_2. Scale bar represents 2 μm. (Bottom) SEM image of 1.2 μm diameter TiO_2. Scale bar represents 1.5 μm.

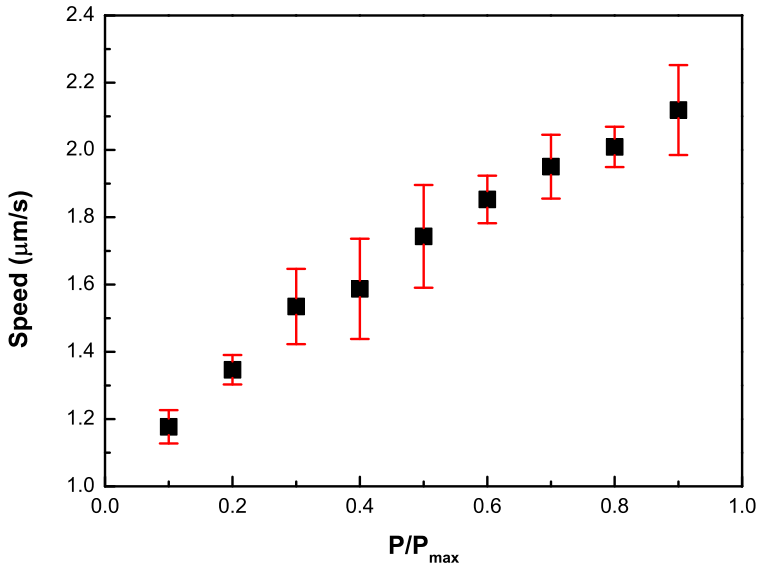

Figure S2. Average speed of self-assembled dimers as a function of the UV light intensity. The maximum light intensity P_{max} is 320 mW/cm^2.

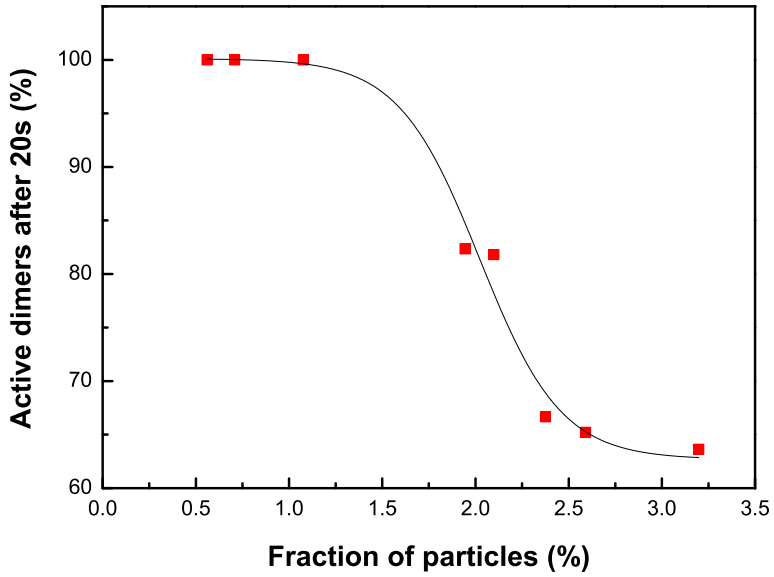

Figure S3. As the number of colloids increases, it is expected that not only dimers form, but also multimers that are more symmetric and less motile. For a fixed active to passive ratio of 3:1 the graph shows the number of active (motile) dimers that survive after 20 *s* as a function of the overall fraction of particles.

Propulsion as a function of ionic strength

The ionic effects that may be involved in the self-assembling and self-propelling mechanisms can be examined by dissolving salt in the systems and changing the concentrations. [1] We perform the experiments with Janus particles (SiO_2 spheres half coated by TiO_2). [2] Figure S4 presents the average speed of the Janus particle as a function of the $NaCl$ concentration. The propulsion speed does not change significantly over a broad range of $NaCl$ concentrations, except at high concentrations (~1 mM) where the chemical activity of the TiO_2 particles is reduced (due to the reduction of the reaction rates). This result implies that diffusiophoresis is a dominant propulsion mechanism in our system.

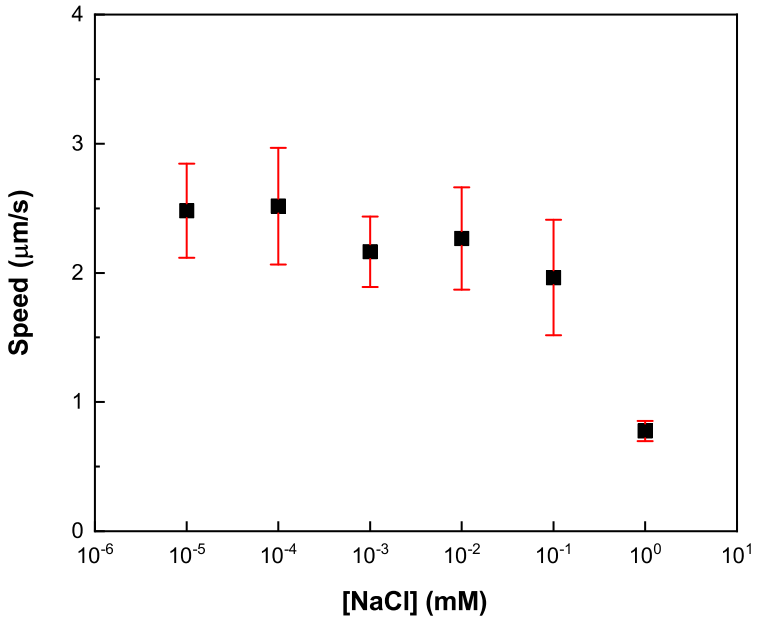

Figure S4. Average speed of 2 μm TiO_2_SiO_2 Janus particle as a function of concentration of $NaCl$.

Simulation Methods

In our simulations, we take a hybrid method combining molecular dynamics (MD) [3] and multiparticle collision dynamics (MPCD) to describe the motions of the colloid and fluid particles, respectively.

In MPCD, the fluid is comprised of N_s point particles of mass m with positions $r_i(t)$ and velocities $v_i(t)$ at time t, where $i = 1,...,N_s$. Chemical species *A* and *B* constitute parts of these fluid particles. Fluid particles have no explicit intermolecular potentials and their interactions are governed by multiparticle collisions. The dynamics consists of two alternating steps, streaming and collision. In the streaming step, the particles move according to Newton's equations of motion with time intervals *h,* called the collision time, and the positions of the particles are updated by $r_i(t+h) = r_i(t) + hv_i(t)$. After the collision time, the solvent particles are sorted into cubic cells of side length *a*, which is larger than the mean free path, and their relative velocities are rotated around a randomly oriented axis by a fixed angle α with respect to the center-of-mass velocities of each cell. The particle velocity after collision is obtained by $v_i(t+h) = v_{cm}(t) + R(\alpha)\big(v_i(t) - v_{cm}(t)\big)$, where $R(\alpha)$ is the rotation matrix, $v_{cm} = \sum_{j=1}^{N_c} v_j / N_c$ is the center-of-mass velocity of the particles in the cell to which the particle *i* belongs, and N_c is the number of particles in that cell. A random shift of the collision lattice is applied at every collision step to ensure Galilean invariance. [4] In this algorithm, momentum and energy are locally conserved and the velocity of the fluid particles follows a Maxwell-Boltzmann distribution. [5]

All quantities are reported in dimensionless units where length, energy, mass and time are measured in units of the MPC cell length $a = \sigma_a/2$, where σ_a is the distance parameter of the catalytic sphere, the energy parameter of the solvent particle ϵ, the solvent mass *m*, and $a\sqrt{m/\epsilon}$, respectively. We choose the simulation box of size $L_x = L_y = 50$ and $L_z = 30$. Multiparticle collisions are carried out by performing velocity rotations by an angle $\alpha = 120°$ about randomly chosen axes in the collision time $h = 0.1$. The average solvent number density is $c_0 = 10$ and the temperature is $k_BT = 1$. The MD time step is $\Delta t = 0.01$. The energy parameters for the S_p sphere and chemicals *A* and *B* in repulsive Lennard-Jones potentials are $\epsilon_A = 1.0$ and $\epsilon_B = 0.1$, respectively, while $\epsilon_A = \epsilon_B = 1.0$ for the S_a sphere. The size parameters are $\sigma_a = 2$ and $\sigma_p = 4$ to give the radii of S_a and S_p spheres are $R_a = 2^{1/6}\sigma_a$ and $R_p = 2^{1/6}\sigma_p$, respectively. The two spheres have excluded volume interactions with $\sigma_S = 6$. The mass of the sphere is taken to be $M = 4\pi\sigma^3 c_0/3$ and neutrally buoyant. The intrinsic reaction rate constant can be estimated from simple collision theory to give $k_0 \sim \sqrt{k_BT/2\pi m} \sim 0.4$. The motions of spheres are confined in the plane parallel to the wall with the force constant $k_c = 10$. The spheres are near the bottom wall with distance $2\sigma_p$ and separated from the upper wall with distance $6.5\sigma_p$ so that hydrodynamic effects from the upper wall are negligible. Periodic boundary conditions are applied in the directions of the motion of the spheres and reflecting boundary conditions are employed in the vertical directions. The transport properties of the fluid depend on h, α, and N_C. The fluid viscosity of $\bar{\mu} = mN_C\nu = 7.9$, where ν is the kinematic viscosity, and the diffusion constant of $D = 0.0611$ ensures a large Schmidt number $S_c = \nu/D = 13 > 1$, which indicates that momentum transport dominates over mass transport, as is characteristic of the liquid state. The low Reynolds number $R_e = c_0V_a/\bar{\mu} < 0.1$, implies that the viscosity is dominant over inertia, and a small $P_e = V_a/D < 1$, means that diffusion is dominant over fluid advection.

Dynamics of two particles

Fig. S5 presents the separation distance of two particles as a function of time.

Fig. S6 shows the capture time as a function of the separation distance. The capture time refers to the time it takes for two spheres that are initially a distance L apart to meet. As shown in Fig. 5 in the main text, the velocity of particles along the separation distance is not linear so that the capture time increases also nonlinearly with the separation distance. [6]

In the main text, we discussed the velocity of catalytic and non-catalytic spheres as a function of their separation distance (Fig. 5). There the interaction energy of chemical species A and B with the catalytic sphere is taken to be the same for convenience ($\varepsilon_A^{cat} = \varepsilon_B^{cat}$). Here we take the different interaction energy to see this change induces the variation of particles dynamics. Three energy parameter sets are considered, $\varepsilon_A^{cat} = \varepsilon_B^{cat} = 1$, $\varepsilon_A^{cat} = 1 > \varepsilon_B^{cat} = 0.1$, and $\varepsilon_A^{cat} = 0.1 < \varepsilon_B^{cat} = 1$ while the interaction potentials with the non-catalytic sphere remains unchanged ($\epsilon_A = 1 < \varepsilon_B = 0.1$). From these energy parameters, the non-catalytic sphere moves toward the catalytic sphere by diffusiophoresis as before. As shown in Fig. S7, the velocity of the catalytic and non-catalytic sphere is not affected by the change of the interaction energy in the catalytic sphere. The minor change in very short separation may arise from the disturbance of homogeneous concentration distributions in the vicinity of the catalytic spheres.

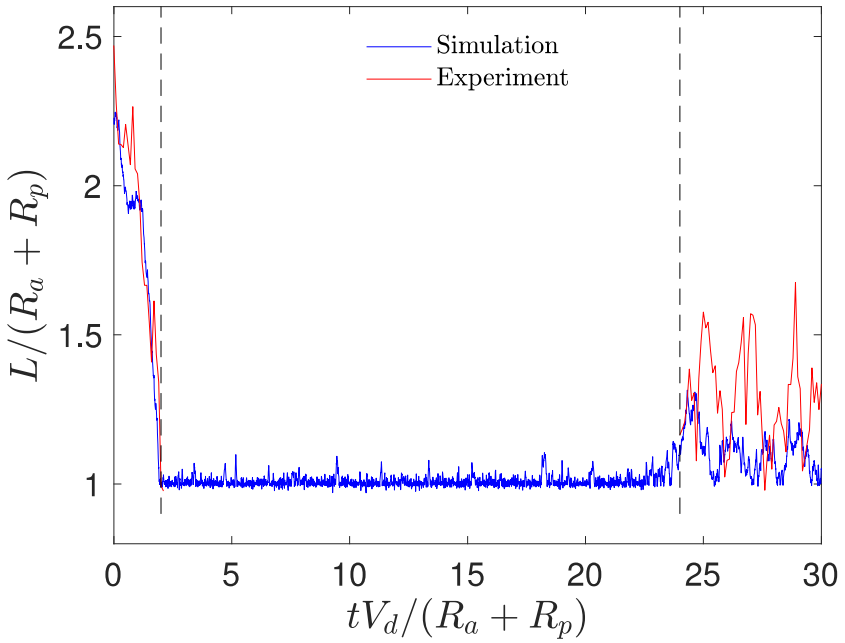

Figure S5. The separation distance of two spheres as a function of time. When the light is switched on, nearby catalytic and non-catalytic monomer particles approach each other and meet to form a dimer. The dimer self-propels stably with a constant velocity V_d. When the light is switched off, the dimer is split into two monomers, which undergo Brownian motion. See also simulation snapshots in Fig. 3 in the text and Movie S2.

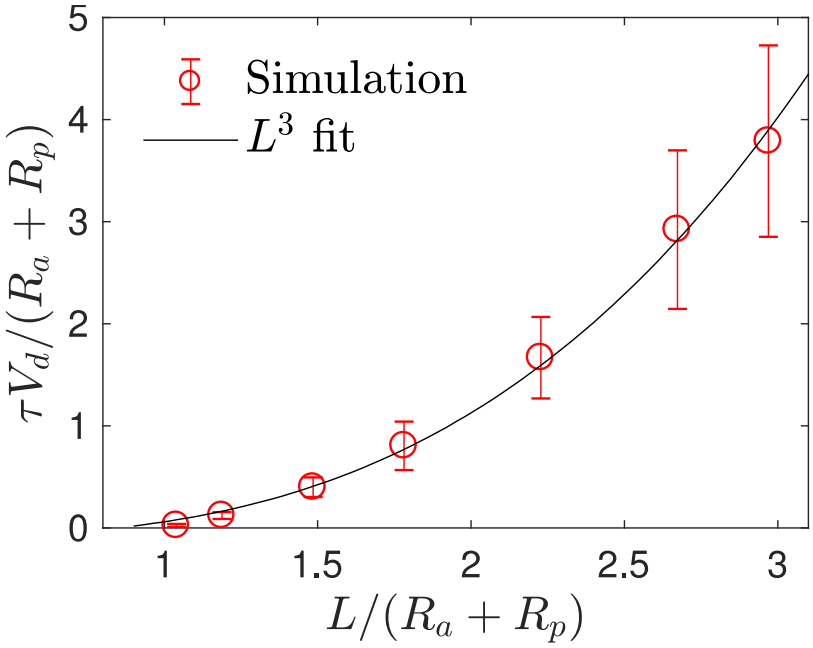

Figure S6. Capture time, which is the time it takes for two spheres that are initially a distance L apart, to meet, as a function of the initial separation distance.

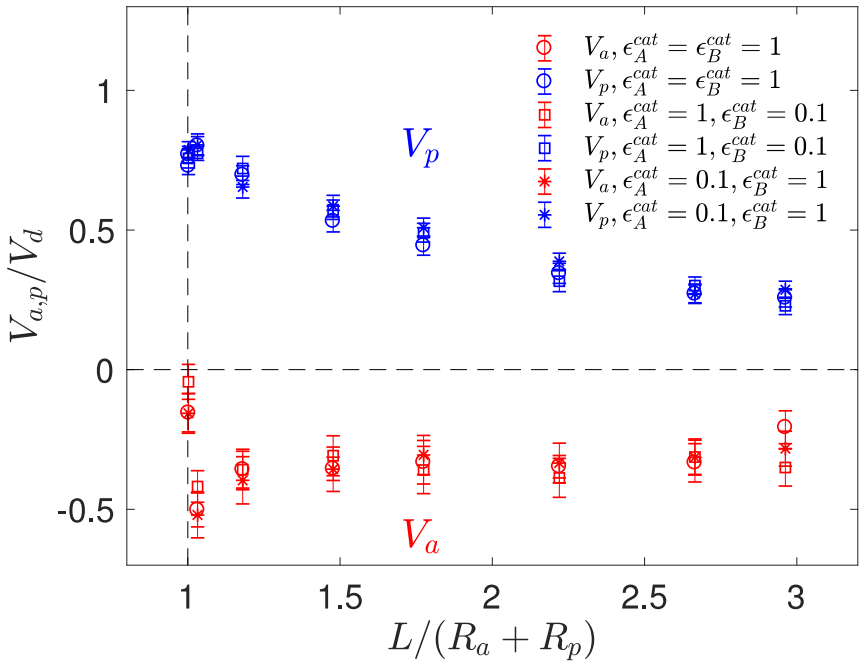

Figure S7. The velocity of catalytic V_a and non-catalytic sphere V_p as a function of separation distance L; the effects on the change of the interaction potentials of chemicals with the catalytic spheres. Three energy parameter sets are considered, $\varepsilon_A^{cat} = \varepsilon_B^{cat} = 1$, $\varepsilon_A^{cat} = 1 > \varepsilon_B^{cat} = 0.1$, and $\varepsilon_A^{cat} = 0.1 < \varepsilon_B^{cat} = 1$ while the interaction potentials with the non-catalytic sphere remains unchanged ($\varepsilon_A = 1 > \varepsilon_B = 0.1$).

Supplementary Videos

Supporting Movie S1: The movie shows experiment results for dimer formation of TiO_2 and SiO_2 colloids and its propulsion under UV illumination. The particles are immersed in an aqueous solution of 1.5 % H_2O_2 and 1 mM TMAH (tetramethylammonium hydroxide). The movie is sped up by 1.5 times.

Supporting Movie S2: The movie shows experimental results that TiO_2 and SiO_2 colloids do not form a dimer in pure water. The movie is sped up by 2 times.

Supporting Movie S3: The movie shows simulation results for dimer formation and propulsion from active and passive spheres by diffusiophoretic mechanisms.

Supporting Movie S4: The movie shows experimental results for the deflection of dimers in an arrangement of active TiO_2 colloids. The movie is sped up by 1.5 times.

Supporting Movie S5: The movie shows simulation results for the deflection of a dimer in an arrangement of active spheres.

Supporting Movie S6: The movie shows experimental results for dimer formation of TiO_2 and PS (polystyrene) and its propulsion. The particles are immersed in an aqueous solution of 1.5 % H_2O_2 and 1 mM TMAH. The movie is sped up by 3 times.

References

1. A. Brown and W. Poon, *Soft Matter*, 2014, **10**, 4016.
2. D. P. Singh, U. Choudhury, P. Fischer, and A. G. Mark, *Adv. Mater.*, 2017, **29**, 1701328.
3. D. Frenkel, and B. Smit, *Understanding Molecular Simulation-From Algorithms to Applications*, San Diego: Academic Press, 1996.
4. T. Ihle and D. M. Kroll, *Phys. Rev. E,* 2001, **63**, 020201(R).
5. A. Malevanets and R. Kapral, *J. Chem. Phys*., 1999, **110**, 8605; ibid., 2000, **112**, 72609. For reviews, see, R. Kapral, *Adv. Chem. Phys.*, 2008, **140**, 89; G. Gompper, T. Ihle, D. M. Kroll and R. G. Winkler, *Adv. Polym. Sci.*, 2009, **221,** 1.
6. S. Y. Reigh, P. Chuphal, S. Thakur, and R. Kapral, *Soft Matter*, 2018, **14**, 6043.